0026-895X/98/020213-08$3.00/0

MOLECULAR PHARMACOLOGY, **53:**213–220 (1998).

S16020–2, a New Highly Cytotoxic Antitumor Olivacine Derivative: DNA Interaction and DNA Topoisomerase II Inhibition

SANDRINE LE MÉE, ALAIN PIERRÉ, JUDITH MARKOVITS, GHANEM ATASSI, ALAIN JACQUEMIN-SABLON, and JEAN-MARIE SAUCIER

Unité de Recherche Associée au Centre National de la Recherche Scientifique 147, Institut Gustave Roussy, 94805 Villejuif Cedex, France (S.L.M., J.M., A.J.-S., J.-M.S.), and Institut de Recherches Servier, Division de Cancérologie Expérimentale, 92150 Suresnes, France (A.P., G.A.)

Received August 4, 1997; Accepted October 6, 1997

This paper is available online at http://www.molpharm.org

ABSTRACT

S16020–2 (NSC-659687) is a new olivacine derivative that is highly cytotoxic *in vitro* and displays remarkable antitumor activity against various experimental tumors, especially some solid tumor models. Its antitumor activity is notably higher than that of 2-methyl-9-hydroxy-ellipticinium (NMHE) and comparable to that of doxorubicin HCl, although with a different tumor specificity. S16020–2 is being tested in phase I clinical trials. A study of the interaction of S16020–2 with DNA showed that it binds through intercalation between adjacent DNA base pairs, inducing an unwinding of 10° of the double helix. Its DNA affinity is approximately equal to that of NMHE and decreases as a function of the salt concentration, indicating a significant electrostatic contribution to the overall binding free energy. S16020–2 did not interfere with the catalytic cycle of DNA topoisomerase I but stimulated DNA topoisomerase II-mediated DNA cleavage via a strictly ATP-dependent mechanism. The interactions of S16020–2 and NMHE with DNA topoisomerase II *in vitro* are very similar. Both drugs have the same DNA sequence specificity of cleavage and the same biphasic dose-effect response, and neither drug inhibited the rate of DNA religation. In contrast with these observations, in *in vivo* experiments, S16020–2 was able to induce topoisomerase II-mediated DNA strand breaks at concentrations 500-fold lower than NMHE. We conclude that DNA topoisomerase II most likely is the cellular target involved in the mechanism of cytotoxicity of S16020–2. Its higher biological activity and potency to induce cellular DNA cleavage suggest the involvement of as-yet-unidentified cellular factors.

Among a new series of 6*H*-pyrido[4,3-*b*]carbazole derivatives, characterized by a basic *N*-dialkylaminoalkyl carboxamido side chain grafted onto an olivacine chromophore (Jasztold-Howorko *et al*., 1994), some derivatives were found to display a remarkable antitumor activity against murine P388 leukemia and colon 38 adenocarcinoma. The most active of these compounds, S16020–2 [9-hydroxy-5,6-dimethyl-1-[*N*-[2(dimethylamino)ethyl]carbamoyl]-6*H*-pyrido-[4,3-*b*]carbazole; NSC 659687] (Fig. 1), was selected for further studies.

The pharmacological activity of S16020–2 was evaluated *in vivo* against several murine tumors, including P388 lymphocytic leukemia, B16 melanotic melanoma, Lewis lung carcinoma, and M 5076 reticulosarcoma, and a panel of human tumor xenografts (Guilbaud *et al*., 1996, 1997; Krauss-Berthier *et al*., in press).The results of these studies indicated that S16020–2 was a much more active antitumor agent than other compounds in the ellipticine series, such as NMHE, and that it compared favorably with Adriamycin. For the tested murine and human cell lines, the cytotoxicity of S16020–2 was more than 40-fold higher than that of NMHE (Léonce *et al*., 1996). At cytotoxic concentrations, S16020–2 induced cells to accumulate in the G2 + M phase. In addition, the drug retained its activity on several P388 leukemia sublines expressing the multidrug resistance phenotype.

Recently, using the COMPARE pattern recognition program to analyze the National Cancer Institute *In Vitro* Antineoplastic Drug Screen database, which contains the differential sensitivity patterns of 60 tumor cell lines to >45,000 compounds, Koo *et al*. (1996) identified S16020–2 as one of four drugs displaying a preferential toxicity on tumor cells harboring activated *ras* oncogenes. This differential sensitivity was confirmed by further testing on a panel of 22 non-small cell lung carcinoma lines, 12 with a mutated *ras* and 10

This work was supported in part by grants from Agence Nationale de Valorisation de la Recherche, Association pour la Recherche sur le Cancer, Fondation pour la Recherche Médicale, and Ligue Nationale contre le Cancer. J.-M. S. was supported by Institut National de la Santé et de la Recherche Médicale.

ABBREVIATIONS: NMHE, 2-*N*-methyl-9-hydroxy-ellipticinium; bp, base pair(s); SSB, single-strand breaks; CD, circular dichroism; DPC, DNA/protein cross-link; HEPES, 4-(2-hydroxyethyl)-1-piperazineethanesulfonic acid; SDS, sodium dodecyl sulfate.

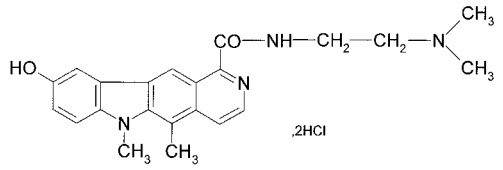

Fig. 1. Structure of S16020–2.

with a wild-type *ras*. Finally, the hematological toxicity of S16020–2 administered to B6D2F1 mice seemed to be less severe than that of doxorubicin HCl (Adriamycin), particularly on bone marrow stem cells (Guilbaud *et al*., 1996). All these observations made S16020–2 a very promising experimental antitumor agent (it was recently introduced in phase I clinical trials) and prompted us to analyze its mechanism of action. Because of its structural analogy with ellipticines, the first logical step of this analysis was to study the interactions of S16020–2 with DNA and DNA topoisomerases.

Materials and Methods

Drugs. S16020–2 was synthesized at Institut de Recherches Servier (Suresnes, France), as described previously (Jasztold-Howorko *et al*., 1994), and its purity was controlled with the use of high performance liquid chromatography. NMHE was supplied as Ellipticinium Acetate by Pasteur Mérieux (Lyon, France). S16020–2 and NMHE were dissolved in H_2O at a concentration of 10 mM. Camptothecin and etoposide (Sigma Chemical, Poole, Dorset, UK) were dissolved in dimethylsulfoxide at a concentration of 10 mM.

Nucleic acids and enzymes. Closed circular plasmid pSP65 DNA (3005 bp) was purified from *Escherichia coli* ATY 0404 (hsdR, hsdM, recA 13) (Lambert *et al*., 1989) through standard procedures. Calf thymus DNA and plasmid pBR322 DNA were purchased from Boehringer-Mannheim Biochemica (Mannheim, Germany). Poly(dA/dT)·poly(dA/dT) was provided by Pharmacia (Uppsala, Sweden). DNA topoisomerase I was purified from calf thymus as described by Liu and Miller (1981). Yeast DNA topoisomerase II was overexpressed in yeast strain DBY745 transformed with YEpTOP2-PGAL1 and purified to near-homogeneity according to the procedure of Worland and Wang (1989).

Absorption and CD measurements. UV absorption measurements were carried out with a spectrophotometer (Uvikon model 941; Kontron Instruments, Montigny-le-Bretonneux, France). CD spectra were recorded with a Jobin-Yvon model Mark IV dichrograph (Longjumeau, France). Absorbance titration experiments were carried out as described previously (Chaires *et al*., 1982). The concentrations of free and DNA bound S16020–2 were determined using extinction coefficient values at 326 nm of 1.205×10^4 and 2.066×10^4 M^{-1} cm^{-1}, respectively. The binding data were analyzed according to the neighbor exclusion model characterized by binding isotherms of the following equation:

$$v/c_f = K_i(1 - nv)\{(1 - nv)/[1 - (n - 1)v]\}^{n-1} \quad (1)$$

where c_f is the free drug concentration, v is expressed as mol of bound drug/mol of DNA base pairs, K_i is the intrinsic binding constant, and n is the exclusion parameter expressed in base pairs (McGhee and von Hippel, 1974).

Viscometric measurements. Low-molecular-weight DNA was prepared by ultrasonic treatment of calf thymus DNA followed by digestion with *Neurospora crassa* endonuclease to remove single-strand regions. The effect of S16020–2 on DNA length was analyzed using a capillary viscometer as described by Saucier *et al*. (1971).

DNA unwinding measurements. pSP65 DNA, at a nucleotide concentration of 63 μM, was relaxed to completion in the presence of S16020–2 by incubation at 37° for 30 min with 8 μg/ml DNA topoisomerase I in 0.1 M NaCl, 2 mM $MgCl_2$, 1 mM EDTA, and 10 mM potassium phosphate, pH 6.5. The DNA/drug complexes were dissociated by extraction of the reaction mixture with an equal volume of phenol/chloroform/isoamyl alcohol (25:24:1, v/v/v), and 19-μl samples were fractionated by electrophoresis (3 V/cm) in 1% agarose gels containing 0.4, 0.8, or 1.2 μg/ml chloroquine. The gels were stained with ethidium bromide and photographed under UV light with Ilford FP4 films. The films were scanned with a Joyce-Loebl Chromoscan 3 microdensitometer, and the heights of the peaks (h) corresponding to individual bands resolved in the gels were measured. For a DNA sample relaxed in the absence of ligand, the topoisomer distribution follows the equation derived from Depew and Wang (1975):

$$\ln h = (a/RT) * (L - L_0)^2 - (2a\omega_0/RT) * (L - L_0) + \ln h_0 \quad (2)$$

where R and T are parameters of the classic Boltzmann equation, a is a constant at a given temperature, h_0 is the peak height of a topoisomer with a linking number L_0 arbitrarily chosen as a reference, L is the linking number of a given topoisomer, and ω_0 is the value of $L - L_0$ at the center of the distribution. The parameters of the parabola that fits best the variations of ln h as a function of $L - L_0$ were determined, and an accurate value of ω_0 was deduced. The same procedure was followed to determine the value of ω for the DNA samples relaxed in the presence of various concentrations of S16020–2.

DNA topoisomerase I-mediated DNA cleavage. Circular pBR322 DNA was cleaved with *Eco*RI restriction endonuclease and end-labeled with [α-^{32}P]dATP by standard procedures (Sambrook *et al*., 1989). The labeled DNA was purified by two ethanol precipitations and cleaved with restriction endonuclease *Hin*dIII in two fragments (4334 and 29 bp), each labeled at one end. DNA topoisomerase I cleavage was carried out in a volume of 15 μl at 37° for 15 min. The incubation mixture contained labeled pBR322 DNA fragments (~6×10^4 dpm) and 9.5 μg/ml DNA topoisomerase I in 20 mM Tris·HCl, pH 7.5, 50 mM KCl, 5 mM $MgCl_2$, 0.1 mM EDTA, 0.5 mM dithiothreitol, and 30 μg/ml bovine serum albumin. The reaction was stopped by the addition of SDS and proteinase K at final concentrations of 0.8% and 63 μg/ml, respectively, and the mixture was incubated for an additional 30 min at 50°. After the addition of 10 μl of loading buffer I [0.45 N NaOH, 30 mM EDTA, 15% (w/v) sucrose, 0.1% bromocresol green], samples were analyzed by electrophoresis (2 V/cm) for 20 hr in a 1% agarose gel containing 0.1% SDS in TBE buffer (90 mM Tris-borate, 2.5 mM EDTA). The gel was dried and autoradiographed.

DNA topoisomerase II-mediated DNA cleavage and religation. DNA topoisomerase II cleavage was carried out in a volume of 15 μl at 28° for 6 min. The incubation mixture contained labeled pBR322 DNA fragments (~6×10^4 dpm) and 19 nM yeast DNA topoisomerase II in the cleavage buffer (20 mM HEPES, pH 7.9, 50 mM KCl, 5 mM $MgCl_2$, 0.1 mM EDTA) with 1 mM ATP and 1.3% glycerol. For the analysis of DNA cleavage in the absence of ATP, the enzyme and glycerol concentrations were 95 nM and 6.7%, respectively. The reaction was stopped by the addition of SDS, and proteinase K digestion was carried out as above. After the addition of 2 μl of loading buffer II (150 mM EDTA, 50% glycerol, 0.4% bromphenol blue, 0.4% xylene cyanol), samples were analyzed by electrophoresis (2 V/cm) for 20 hr in a 1.2% agarose gel in TBE buffer containing 0.1% SDS.

Religation assays were performed as described (Froelich-Ammon *et al*., 1995) using 50 nM DNA topoisomerase II and 5 nM pBR322 DNA. DNA cleavage/religation equilibrium was established in the cleavage buffer in the presence of 3.5% glycerol and 1 mM ATP, and DNA religation was induced by rapidly shifting samples from 28° to either 55° or 65°. After varying time intervals, religation was terminated by the addition of 2 μl of 10% SDS. After proteinase K digestion at 50° for 30 min., 2 μl of loading buffer II was added, and the samples were heated at 68° for 2 min. Reaction products were fractionated by electrophoresis in 1% agarose gels in TBE buffer containing 0.5 μg/ml ethidium bromide. The amount of cleaved linear DNA was quantified by scanning the gel with a Bioprofil Scan (Vilbert Lourmat, Marve-la-Vallée, France).

Cell line and cell survival. The Chinese hamster lung cell line DC-3F was maintained as described previously (Khélifa *et al*., 1994). The *in vitro* colony formation assay was used to determine the cell survival fraction after drug exposure. Exponentially growing cells (2.5×10^5) were grown in 60-mm-diameter Petri dishes (Falcon, Beckton Dickinson, Plymouth, UK) for 18 hr at 37° before drug treatment. After 3 hr of exposure to S16020–2 or NMHE, the cells were trypsinized, and appropriate dilutions were made to seed 250 treated cells onto 60-mm Petri dishes. Colonies were stained and counted 7 days later.

Measurements of DNA damage by alkaline elution. DNA SSB were assayed by DNA denaturing alkaline elution carried out under deproteinizing conditions (Kohn *et al*., 1981). Briefly, cellular DNA in exponentially growing DC-3F cells was labeled for 20 hr at 37° by the addition to the culture medium of 0.02 μCi/ml [2-^{14}C]thymidine (Amersham International, Buckinghamshire, UK) or 0.1 μCi/ml [*methyl*-^{3}H]thymidine (Amersham). After removal of the medium, the cells were grown for at least 2 hr in label-free medium before all experiments. ^{14}C-Thymidine-labeled cells were treated with the drug at increasing concentrations for 1 hr. Drug treatments were terminated by removal of the drug-containing medium and resuspension of the cells in ice-cold Hanks' balanced salt solution containing 0.02% EDTA. ^{14}C-Labeled cells were mixed with untreated ^{3}H-labeled cells (internal standard) that had been irradiated with 1000 rads. Cells were maintained in ice until being assayed by alkaline elution. Drug-induced SSB were compared with γ-ray-induced SSB and expressed as the radiation dose that would produce the same frequency of that type of break.

DPCs were assayed by DNA denaturing alkaline elution carried out under nondeproteinizing conditions using protein-absorbing filters (polyvinyl chloride; Gelman Sciences, Ann Arbor, MI) (Kohn *et al*., 1981). Both ^{14}C- and ^{3}H-labeled cells were γ-irradiated in ice with 3000 rads just before elution. DPC frequencies were calculated as described by Ross *et al*. (1979).

Results

Absorption and CD analysis of S16020–2 interaction with poly(dA/dT)·poly(dA/dT). Marked changes in the UV absorption spectrum of S16020–2 in aqueous solution occurred on the addition of poly(dA/dT)·poly(dA/dT), as shown in Fig. 2A. The λ_{max} of the absorption band of the free drug gradually shifted from 307 nm to ~313 nm, whereas a hypochromic effect was induced below 317 nm. The observation of an isobestic point at 317 nm suggested the existence of two forms of the drug in equilibrium, free and bound to the polynucleotide, allowing the analysis of the binding of S16020–2 to nucleic acids by absorbance titration experiments as shown below.

S16020–2 is an achiral molecule, so the chromophore of the free drug displayed no CD in the wavelength range of its absorption spectrum (230–360 nm). Uncomplexed poly(dA/dT)·poly(dA/dT) displayed a positive signal at 262 nm and a negative signal at 250 nm, which are typical features of B DNA. On the addition of S16020–2 to a solution of the polynucleotide, significant changes in its CD spectrum were observed (Fig. 2B): the negative band shifted from 250 to 257 nm, whereas the positive signal disappeared gradually. Such changes are likely to result from structural alterations induced by the drug into the polynucleotide bihelical structure. In addition, a positive signal appeared in the range of 310 to 350 nm, in which poly(dA/dT)·poly(dA/dT) does not absorb light. This signal reflects asymmetrical structural changes induced in the drug chromophore on binding to the nucleic acid. The symmetry of the positive CD signal in the range of 310 to 350 nm suggests the existence of a single mode of drug/polynucleotide interaction, most likely an intercalation of S16020–2 between adjacent base pairs.

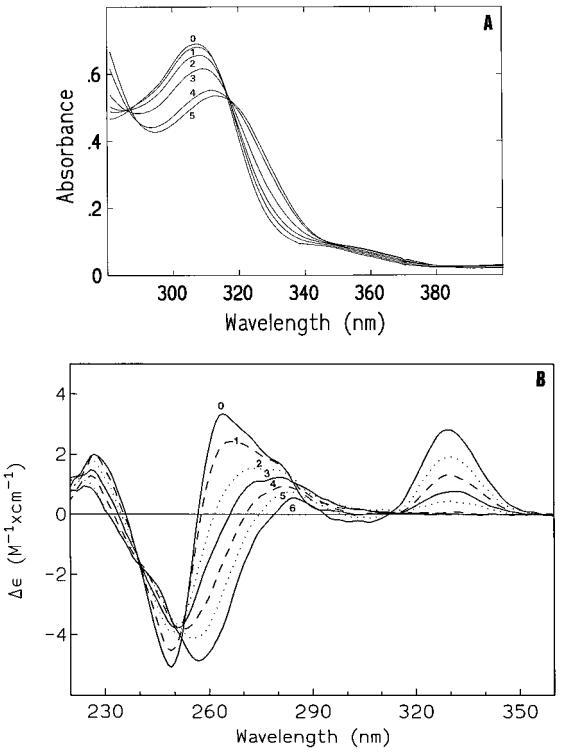

Fig. 2. UV absorption and CD spectra of S16020–2 in the presence of poly(dA/dT)·poly(dA/dT). A, Absorption spectra of 25 μM S16020–2 in 0.25 M NaCl, 1 mM EDTA, and 10 mM sodium cacodylate, pH 6.5, were recorded at 20° in 1-cm path-length cuvettes in the absence of polynucleotide (*0*) or in its presence (*1–5*). Drug/nucleotide molar ratios were 2.38 (*1*), 1.19 (*2*), 0.60 (*3*), 0.30 (*4*), and 0.24 (*5*). B, CD spectra at 20° in 1-cm path-length cuvettes of 75 μM polynucleotide and various concentrations of S16020–2. Drug/nucleotide molar ratios were 0 (*0*), 0.066 (*1*), 0.15 (*2*), 0.20 (*3*), 0.27 (*4*), 0.33 (*5*), and 0.47 (*6*).

Analysis of S16020–2 binding to DNA. The binding of S16020–2 to calf thymus DNA was analyzed quantitatively by absorbance titration of the DNA with the drug at three salt concentrations. K_i and n values providing the best fit of experimental data to eq. 1 were selected and appear in Table 1. The corresponding binding isotherms are plotted in Fig. 3. The DNA/S16020–2 binding constant decreases as a function of Na^+ concentration, with a slope $d(\log K_i)/d(\log Na^+) = 1.0$, indicating the release of one monovalent cation from the DNA on binding of one molecule of S16020–2 (Chaires, 1996). At the three salt concentrations studied, the exclusion parameter is constant and found to be equal to an average of 2.44 bp, supporting the hypothesis of an intercalation mode of binding according to the neighbor exclusion model. The

TABLE 1
DNA binding constants of S16020-2 and NMHE determined at 20°

[NaCl]	S16020-2		NMHE	
	K_i	n	K_i	n
M	M^{-1}	bp	M^{-1}	bp
0.10	1.43×10^6	2.44	N.D.	N.D.
0.25	9.12×10^5	2.44	7.87×10^5	2.26
0.50	2.71×10^5	2.43	2.44×10^5	2.14

K_i and n are defined in Materials and Methods. N.D., not determined.

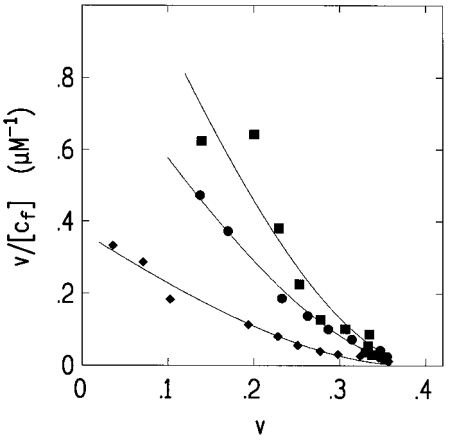

Fig. 3. Spectrophotometric analysis of S16020–2 binding to DNA. Measurements were carried out at 326 nm at 20° in 1-cm path-length cuvettes containing 49.5 μM calf thymus DNA base pairs in 10 mM sodium cacodylate, pH 6.5, 1 mM EDTA, and 0.1 M (■), 0.25 M (●), or 0.5 M (♦) NaCl. A solution of 275 μM S16020–2 was added stepwise to final concentrations of 23–30 μM. *Solid lines*, best fit of the experimental data to the McGhee and von Hippel equation.

DNA/S16020–2 binding constants were compared with the DNA/NMHE binding constants determined under identical conditions according to the same absorbance titration method. As indicated in Table 1, the binding constants of S16020–2 are very similar to those of NMHE.

The ability of S16020–2 to intercalate between DNA base pairs was studied by viscometric analysis of the effect of the drug on the length of short DNA rods obtained through ultrasonic treatment of calf thymus DNA. Data plotted in Fig. 4 show that log ($[\eta]/[\eta_0]$) varies linearly as a function of log(1 + v), which indicates a linear increase in DNA length as a function of the amount of bound drug. The slope of the straight line drawn in Fig. 4 is equal to 2.5, which is a typical value observed with DNA intercalating compounds (Saucier *et al.*, 1971).

The DNA helix unwinding angle induced by S16020–2 intercalation was determined by measuring the linking number decrease on a closed circular plasmid DNA molecule relaxed in the presence of increasing concentrations of the drug. From the data plotted in Fig. 5, an unwinding angle of 10.2°/intercalated molecule was calculated.

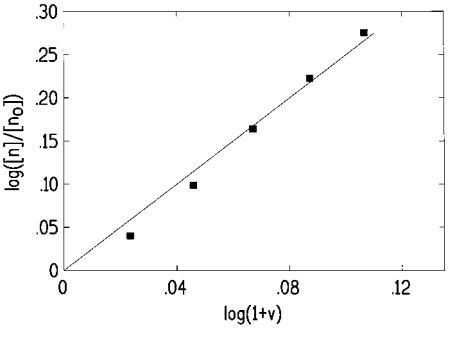

Fig. 4. Viscometric analysis of the length variation of sonicated DNA induced by S16020–2. Measurements were carried out at 25° in solution containing 345 μM DNA base pairs, 0.1 M NaCl, 1 mM EDTA, 0.1 M Tris·HCl, pH 7.5, and S16020–2 at concentrations of 0–100 μM. The number of S16020–2 molecules bound/DNA base pair (v) was calculated with the assumption that the drug was quantitatively bound to DNA. [η_o] and [η] are the intrinsic viscosities of free DNA and DNA/drug complex, respectively.

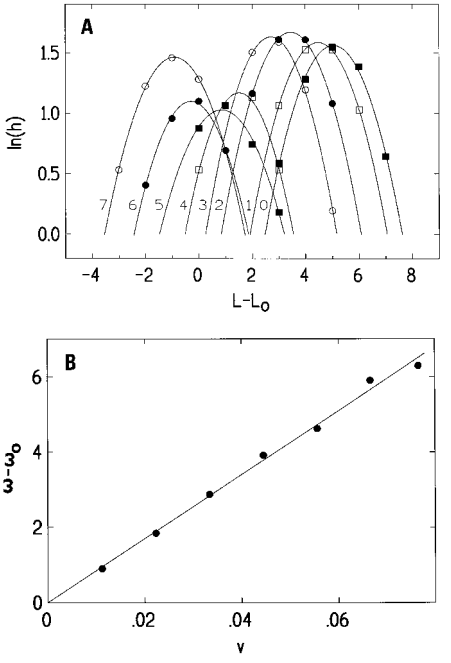

Fig. 5. Unwinding of pSP65 DNA by S16020–2. A, The topoisomer distribution of closed circular pSP65 DNA relaxed by DNA topoisomerase I in the presence of S16020–2 at different concentrations was analyzed by agarose gel electrophoresis as described in Materials and Methods. The amount of drug molecules bound/DNA base pairs (v) was calculated for each sample using the binding parameters values taken from Table 1: no drug (*0*), 1.12×10^{-2} (*1*), 2.23×10^{-2} (*2*), 3.34×10^{-2} (*3*), 4.45×10^{-2} (*4*), 5.56×10^{-2} (*5*), 6.66×10^{-2} (*6*), and 7.66×10^{-2} (*7*). B, Variations of linking number as a function of v for the different DNA samples analyzed.

Interaction of S16020–2 with DNA topoisomerases. The cytotoxicity of several classes of DNA intercalating compounds results from their ability to convert topoisomerases into cellular poisons (Liu, 1989). These agents trap a transient enzyme/DNA covalent complex formed during the catalytic cycle of the enzyme. In this complex, termed cleavable complex, a tyrosine residue of the enzyme is bound to a phosphate of the DNA through a transesterification reaction that creates an interruption of the phosphodiester backbone. To determine whether S16020–2 interacts with DNA topoisomerases via such a mechanism, we studied its effect on topoisomerase I- and II-mediated DNA cleavage *in vitro* with the use of purified enzymes (Fig. 6). A linear end-labeled DNA molecule was incubated with DNA topoisomerase I in the presence of S16020–2 at increasing concentrations. Camptothecin (10 μM) was used as a control. The cleavage patterns observed after agarose gel electrophoresis of the reaction products indicate that S16020–2, up to a concentration of 50 μM, did not stimulate DNA topoisomerase I-mediated DNA cleavage (Fig. 6A).

Using the same substrate, the effect of S16020–2 on DNA topoisomerase II-mediated DNA cleavage was examined in the presence of ATP. As shown in Fig. 6B, S16020–2 clearly stimulated DNA cleavage. Cleavage patterns induced by S16020–2 and NMHE are identical, indicating that the two drugs have the same DNA sequence specificity of cleavage. Some of these NMHE-induced cleavage sites (Fig. 6B, *A–F*) were identified and sequenced previously (Fossé *et al.*, 1991). In addition, the same biphasic dose-effect response described for NMHE (Fossé *et al.*, 1992) was observed with S16020–2, with a maximum at ~8 μM.

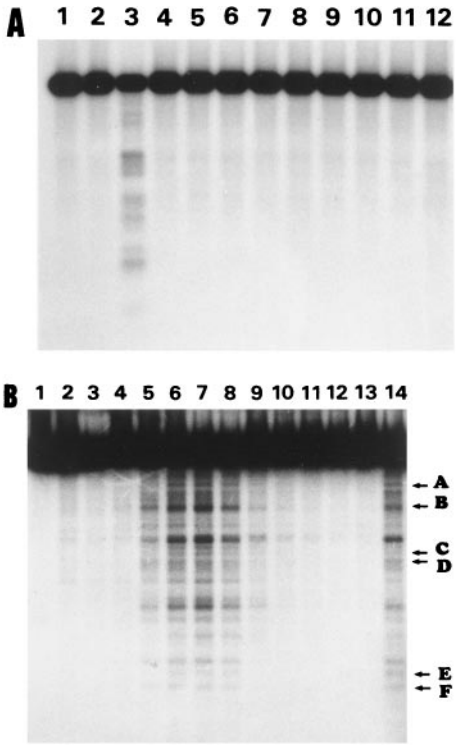

Fig. 6. Effect of S16020–2 on the DNA topoisomerase-mediated DNA cleavage. Reactions were carried out as described in Materials and Methods. A, DNA topoisomerase I-mediated cleavage. *Lane 1*, pBR322 DNA substrate without enzyme or drug. *Lane 2*, control with 10% dimethylsulfoxide. *Lane 3*, cleavage in the presence of 10 μM camptothecin. *Lane 4*, control without drug. *Lanes 5–12*, cleavage in the presence of S16020–2 at concentrations of 1 μM (*lane 5*), 2 μM (*lane 6*), 4 μM (*lane 7*), 8 μM (*lane 8*), 12 μM (*lane 9*), 16 μM (*lane 10*), 20 μM (*lane 11*), and 50 μM (*lane 12*). B, DNA topoisomerase II-mediated cleavage. *Lane 1*, pBR322 DNA substrate without enzyme or drug. *Lane 2*, control without drug. *Lanes 3–13*, cleavage in the presence of S16020–2 at concentrations of 1 μM (*lane 3*), 2 μM (*lane 4*), 4 μM (*lane 5*), 6 μM (*lane 6*), 8 μM (*lane 7*), 10 μM (*lane 8*), 12 μM (*lane 9*), 14 μM (*lane 10*), 16 μM (*lane 11*), 20 μM (*lane 12*), and 25 μM (*lane 13*). *Lane 14*, cleavage in the presence of 2 μM NMHE. Molecular weight standards (not shown) were used to calculate the size of the fragments, and the location of the cleavage sites in the pBR322 map was determined. *A–F*, Positions of NMHE-induced cleavage sites previously identified and sequenced (Fossé *et al.*, 1991).

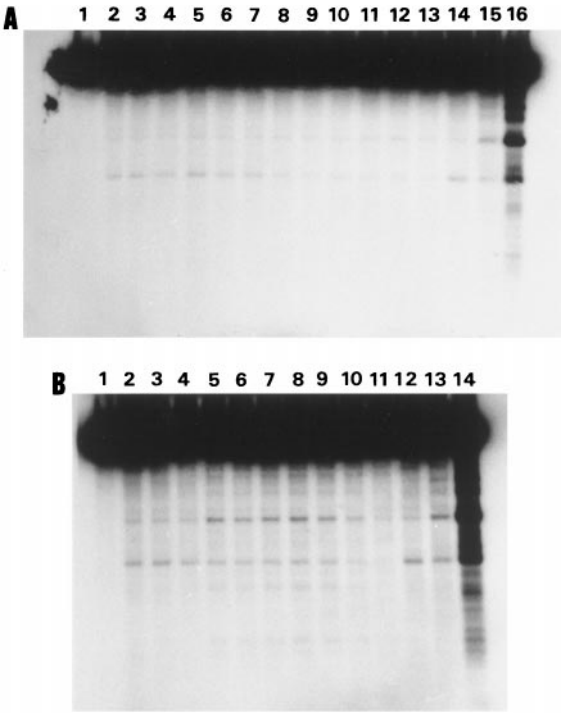

Fig. 7. Effects of S16020–2 (A) and NMHE (B) on the prestrand passage cleavage/religation equilibrium of topoisomerase II. Reactions were carried out in the absence of ATP as described in Materials and Methods. A: *Lane 1*, pBR322 DNA substrate alone. *Lane 2*, cleavage without drug. *Lanes 3–13*, cleavage in the presence of S16020–2 at concentrations of 0.2 μM (*lane 3*), 0.5 μM (*lane 4*), 1 μM (*lane 5*), 2 μM (*lane 6*), 4 μM (*lane 7*), 6 μM (*lane 8*), 8 μM (*lane 9*), 10 μM (*lane 10*), 12 μM (*lane 11*), 16 μM (*lane 12*), and 20 μM (*lane 13*). *Lane 14*, control with 1% dimethylsulfoxide; cleavage in the presence of 10 μM VP-16 (*lane 15*) and 100 μM VP-16 (*lane 16*). B: *Lane 1*, pBR322 DNA substrate alone. *Lane 2*, cleavage without drug. *Lanes 3–11*, cleavage in the presence of NMHE at concentrations of 1 μM (*lane 3*), 2 μM (*lane 4*), 4 μM (*lane 5*), 6 μM (*lane 6*), 8 μM (*lane 7*), 10 μM (*lane 8*), 20 μM (*lane 9*), 30 μM (*lane 10*), and 40 μM (*lane 11*). Lane 12, control with 1% dimethylsulfoxide; cleavage in the presence of 1 μM VP-16 (*lane 13*) and 100 μM VP-16 (*lane 14*).

The effect of ATP on the stimulation of topoisomerase II-mediated DNA cleavage in the presence of enzyme inhibitors is complex, and depending on the particular drug class, ATP may or may not stimulate the reaction (Chen and Liu, 1994). The effect of S16020–2 on the cleavage reaction then was studied in the absence of ATP (Fig. 7). Despite a 5-fold increase in the amount of topoisomerase II in the reaction mixture, in the absence of ATP, there was no detectable stimulation of DNA cleavage by S16020–2 at concentrations ranging from 0.2 to 20 μM. In contrast, when the same experiment was carried out in the presence of 1–40 μM NMHE, a biphasic stimulation of cleavage was observed with a maximum effect at a concentration of ~10 μM. These observations demonstrate that the stimulation of the DNA cleavage reaction by S16020–2 is strictly ATP dependent.

Based on different religation assays (Robinson and Osheroff, 1991; Sorensen *et al.*, 1992; Froelich-Ammon *et al.*, 1995), it was reported that drug-induced increase of the amount of cleavable complexes may involve two different mechanisms: some drugs, including VP-16 (etoposide) and 4′-(9-acridinylamino)methanesulfon-*m*-anisidide (amsacrine), strongly inhibit enzyme-mediated DNA religation, whereas others, like ellipticine, have little effect on religation and presumably act by enhancing the forward rate of cleavage. To determine the mechanism by which S16020–2 stimulates the cleavable complex formation, the effect of the drug on the rate of religation was studied using the heat religation assay described previously (Froelich-Ammon *et al.*, 1995). The DNA cleavage/religation equilibrium was established by incubation at 28° in the presence of 1 mM ATP, and the religation was initiated by shifting the assay mixtures from 28° to a high temperature at which religation rates can be measured without interference of the forward cleavage reaction. Religation kinetics were carried out at 55° or 65°, with similar results. Fig. 8 shows that in agreement with previous observations (Robinson and Osheroff, 1991; Froelich-Ammon *et al.*, 1995), etoposide strongly inhibits DNA religation at 65°, whereas neither S16020–2 nor NMHE alter significantly the apparent first-order rate of the reaction. These results then indicate that S16020–2 and NMHE, like ellipticine (Froelich-Ammon *et al.*, 1995), stimulate enzyme-mediated DNA cleavage by increasing the forward rate of cleavage.

Cytotoxicity of S16020–2 and induction of DNA strand breaks in DC-3F cells. The above results showed that S16020–2 was a DNA topoisomerase II inhibitor that

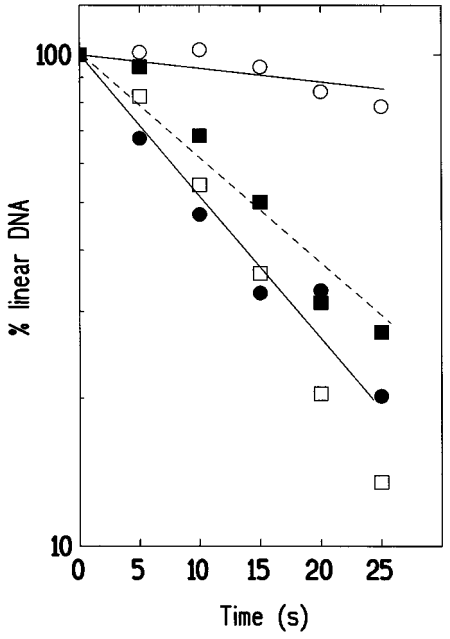

Fig. 8. Effect of S16020–2 and NMHE on the ability of topoisomerase II to mediate DNA religation in the presence of ATP. Religation rates were measured in the presence of 6 μM S16020–2 (□), 2 μM NMHE (■), or 30 μM VP-16 (○) or in the absence of inhibitor (●). Data are plotted in a semilogarithmic fashion as the loss of linear DNA versus time. The proportion of linear DNA for each assay was arbitrarily set to 100% at time zero. Plots represent the average of two independent experiments.

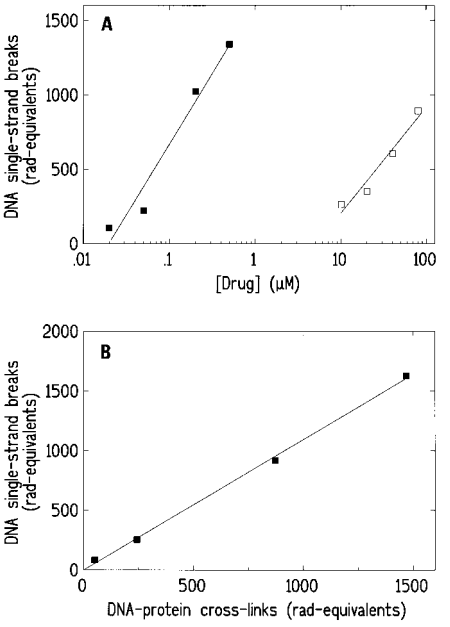

Fig. 9. Induction of DNA breaks in DC-3F cells by S16020–2 and NMHE. A, DC-3F cells were exposed to the indicated concentrations of S16020–2 (■) or NMHE (□) for 1 hr at 37°. Drug then was removed by washing the cell cultures twice with Hanks' balanced salt solution at 0°. Cells were scrapped, and DNA SSBs were measured by DNA denaturing alkaline elution. Data represent the average of two independent experiments. B, Relationship between DNA SSB frequency and DPC frequency in DC-3F cells treated with S16020–2. DNA SSBs were measured as described in A. DPCs were measured by DNA denaturing alkaline elution without proteinase K. *Points*, average of two independent experiments.

was likely to induce enzyme mediated-DNA cleavage in drug-treated cells. Using the alkaline elution assay for measurement of the induction of DNA SSBs, the experiment in Fig. 9A shows that this is indeed the case. In agreement with previous results (Pommier *et al.*, 1986), DNA SSBs are induced by NMHE in intact DC-3F cells in the concentration range of 10–80 μM. Interestingly, S16020–2 also induces DNA SSBs but at concentrations ~500-fold lower than NMHE. Furthermore, all the S16020–2-induced breaks are protein-associated strand breaks (Fig. 9B), which indicates they are all DNA topoisomerase II-associated breaks. The higher capacity of S16020–2 to increase the amount of cleavable complex was associated with a >20-fold higher cytotoxicity in DC-3F cells: the ID_{50} values of S16020–2 and NMHE, determined by the colony formation assay after a 3-hr exposure to the drug, were 33 and 760 nM, respectively.

Discussion

S16020–2 is a new olivacine derivative that has a higher cytotoxicity and better antitumor activity than the ellipticine derivative NMHE, taken here as a reference (Guilbaud *et al.*, 1996). S16020–2 retains its cytotoxicity toward cells expressing the *MDR1* gene (Léonce *et al.*, 1996) and displays an antitumor activity comparable to, but with a spectrum of activity notably different from, that of doxorubicin HCl (Guilbaud *et al.*, 1996, 1997; Kraus-Berthier *et al.*, 1997). In mice, its hematotoxicity at pharmacological doses seemed to be less severe than that of doxorubicin HCl (Guilbaud *et al.*, 1996). For all these reasons, S16020–2 is a very promising new molecule and is under study in phase I clinical trials. The aim of this study was to analyze the physicochemical properties of this new compound in an attempt to understand its superior biological activity.

As expected for an olivacine derivative, S16020–2 binds to DNA, with an affinity comparable to that of NMHE, by intercalation between adjacent base pairs as demonstrated by the results of CD and conformational studies. The DNA unwinding angle of 10.2° induced by intercalation of one S16020–2 molecule is smaller than that of NMHE (21°) and nearly equal to that of the antitumor derivative 2-(diethylamino-2-ethyl)9-hydroxyellipticinium, which, like S16020–2, possesses a positively charged side chain (Auclair *et al.*, 1987). For both compounds, a localization of the charged side chain in the DNA small groove is very likely.

DNA topoisomerase inhibitors constitute a class of antitumor drugs of major clinical importance (Pommier *et al.*, 1996). In this class, ellipticine and olivacine derivatives of pharmacological interest are specific topoisomerase II inhibitors able to stimulate the formation of the drug/enzyme/DNA cleavable complex. In this respect, S16020–2 displays a strong similarity with NMHE. S16020–2 is a specific topoisomerase II inhibitor that stimulates the complex formation in a concentration range close to that of NMHE and according to a dose-effect biphasic process common to all strong intercalators (Liu, 1989). In agreement with previous data in the ellipticine series (Fossé *et al.*, 1992), preliminary studies indicate that both the cytotoxicity and interaction of S16020–2 with topoisomerase II depend on the nature of the substituent in position 9 and structure of the side chain (data not shown). The sequence specificity of the S16020–2-stimulated cleavage sites most likely is identical to that of ellipticine derivatives. Finally, analysis of the kinetics of the

cleavable complex religation shows that S16020–2, as well as ellipticine derivatives, does not change significantly the religation rate and therefore likely stimulates DNA topoisomerase II-mediated DNA cleavage by the same mechanism of enhancement of the forward rate of the cleavage reaction.

However, S16020–2 differs markedly from any other topoisomerase II inhibitor in its absolute ATP requirement to stimulate the enzyme-mediated DNA cleavage. ATP has various effects on cleavable complex formation in the presence of different compounds: all the topoisomerase II inhibitors identified so far were able to induce the complex formation in the absence of ATP, and many of them were stimulated in the presence of ATP. S16020–2 is unique because even when the enzyme concentration had been increased by 5-fold, there was no detectable cleavable complex stimulation in absence of ATP. Topoisomerase II catalytic cycle is known to involve several conformational changes, and some of them are triggered by ATP binding or hydrolysis (Berger *et al*., 1996). One speculation then would be that S16020–2 specifically binds to the enzyme/DNA complex in the conformation induced by ATP binding at an early step of the cycle (Berger *et al*., 1996; Chen and Liu, 1994).

The *in vitro* stimulation of DNA topoisomerase II-mediated DNA cleavage and the induction of protein-associated DNA breaks in DC-3F cells exposed to the drug at cytotoxic concentrations indicate that DNA topoisomerase II is the cellular target mediating the cytotoxic activity of S16020–2. In addition, the DC-3F/9-OH-E cell line, selected for the resistance to 9-OH-ellipticine and cross-resistant to any topoisomerase II inhibitor (*Salles et al*., 1982), also is cross-resistant to S16020–2 (data not shown). Furthermore, from the same parental DC-3F cell line, a subline resistant to S16020–2 has been isolated in our laboratory (S. Le Mée, unpublished observations). This cell line displays cross-resistance to different DNA topoisomerase inhibitors, also supporting the conclusion that DNA topoisomerase II is involved in the mechanism of cytotoxicity of S16020–2.

In contrast with the results obtained in vitro showing very similar properties for S16020–2 and NMHE, S16020–2 was ~20-fold more cytotoxic than NMHE on the DC-3F cell line, and in these cells, the formation of the cleavable complex was detected at concentrations ~500-fold lower than with NMHE. Several hypotheses can be formulated to explain these important *in vivo* differences. First, because all the *in vitro* studies were carried out with the purified α enzyme, a strong specificity of S16020–2 for the β enzyme might account for these results. Recent studies indicate that some topoisomerase II inhibitors, like 4′-(9-acridinylamino)methanesulfon-*m*-anisidide, exhibit in mammalian cells a strong preference for the β isoform, whereas others, like VP 16, are equally active on both enzymes (Dereuddre *et al*., 1997). Alternatively, the *in vivo* stabilization of the ternary drug/enzyme/DNA complex in the presence of S16020–2 might involve in the DC-3F cells a cofactor, which would be absent in the purified yeast topoisomerase II used *in vitro*. Another possible mechanism would be the metabolic transformation of S16020–2, generating more active and cytotoxic products. However, several S16020–2 possible metabolites were identified *in vivo* in rat and monkey and then synthesized. These compounds did not show any significant difference in their potency to stimulate DNA topoisomerase II-mediated DNA cleavage *in vitro* compared with S16020–2 (S. Le Mée, unpublished observations). In addition, we have no experimental evidence showing that they can be generated in cultured tumor cells. Finally, a difference in the intracellular accumulation and/or distribution of S16020–2 and NMHE might account for their different cytotoxicities. Indeed, a fluorescence analysis of the intracellular localization of 2-*N*-methylellipticinium, a fluorescent ellipticine derivative, showed that the drug was very predominantly present in the cytoplasm (Charcosset *et al*., 1983). If the cells concentrate more efficiently S16020–2 in their nucleus, a higher cytotoxicity could be expected.

In conclusion, contrasting with the similarity of their *in vitro* properties, S16020–2 and NMHE markedly differ *in vivo* by the capacity of S16020–2 to stimulate the formation of the topoisomerase II-mediated cleavable complex at concentrations several hundred-fold lower than any other ellipticine or olivacine derivatives characterized so far. An attempt to understand the mechanism underlying this remarkable property of S16020–2, in particular through the characterization of the S16020–2-resistant cells, is in progress in our laboratory.

Acknowledgments

We are grateful to Dr. J. C. Wang for his generous gift of YEpTOP2-PGAL1 plasmid.

References

Auclair C, Pierré A, Voisin E, Pepin O, Cros S, Colas C, Saucier J-M, Verschuere B, Gros P, and Paoletti C (1987) Physicochemical and pharmacological properties of the antitumor ellipticine derivative 2-(diethylamino-2-ethyl)9-hydroxy ellipticinium-chloride, HCl. *Cancer Res* **47:**6254–6261.

Berger JM, Gamblin SJ, Harrison SC, and Wang JC (1996) Structure and mechanism of DNA topoisomerase II. *Nature (Lond)* **379:**225–232.

Chaires JB (1996) Dissecting the free energy of drug binding to DNA. *Anti-Cancer Drug Design* **11:**569–580.

Chaires JB, Dattagupta N, and Crothers DM (1982) Studies on interaction of anthracycline antibiotics and deoxyribonucleic acid: equilibrium binding studies on interaction of daunomycin with deoxyribonucleic acid. *Biochemistry* **21:**3933–3940.

Charcosset J-Y, Salles B, and Jacquemin-Sablon A (1983) Uptake and cytofluorescence localization of ellipticine derivatives in sensitive and resistant Chinese hamster lung cells. *Biochem Pharm* **32:**1037–1043.

Chen AY and Liu LF (1994) DNA topoisomerases, essential enzymes and lethal targets. *Annu Rev Pharmacol Toxicol* **34**:191–218 .

Depew DE and Wang JC (1975) Conformational fluctuations of DNA helix. *Proc Natl Acad Sci USA* **72:**4275–4279.

Dereuddre S, Delaporte C, and Jacquemin-Sablon A. (1997) Role of topoisomerase IIβ in the resistance of 9-OH-ellipticine resistant Chinese hamster fibroblasts to topoisomerase II inhibitors. *Cancer Res* **57:**4301–4308.

Fossé P, René B, Charra M, Paoletti C, and Saucier J-M (1992) Stimulation of topoisomerase II-mediated DNA cleavage by ellipticine derivatives: structure-activity relationship. *Mol Pharmacol* **42:**590–595.

Fossé P, René B, Le Bret M, Paoletti C, and Saucier J-M (1991) Sequence requirements for mammalian topoisomerase II-mediated DNA cleavage stimulated by an ellipticine derivative. *Nucleic Acids Res* **19:**2861–2868.

Froelich-Ammon SJ, Patchan MW, Osheroff N, and Thompson RB (1995). Topoisomerase II binds to ellipticine in the absence or presence of DNA. *J Biol Chem* **270:**14998–15004.

Guilbaud N, Kraus-Berthier L, Saint-Dizier D, Rouillon M-H, Burbridge M, Pierré A, and Atassi G (1997) Antitumor activity of S16020–2 in two orthotopic models of lung cancer. *Anti-Cancer Drugs* **8**:276–282.

Guilbaud N, Kraus-Berthier L, Saint-Dizier D, Rouillon M-H, Jan M, Burbridge M, Visalli M, Bisagni E, Pierré A, and Atassi G (1996) *In vivo* antitumor activity of S16020–2, a new olivacine derivative. *Cancer Chemother Pharmacol* **38:**513–521.

Jasztold-Howorko R, Landras C, Pierré A, Atassi G, Guilbaud N, Kraus-Berthier L, Léonce S, Rolland Y, Prost J-F, and Bisagni E (1994) Synthesis and evaluation of 9-hydroxy-5-methyl- (and 5,6-dimethyl)-6H-pyrido[4,3-b]carbazole-1-N-[(dialkylamino)alkyl]carboxamides, a new promising series of antitumor olivacine derivatives. *J Med Chem* **37:**2445–2452.

Khélifa T, Casabianca-Pignède M-R, René B, and Jacquemin-Sablon A (1994) Expression of topoisomerases II α and β in Chinese hamster lung cells resistant to topoisomerase II inhibitors. *Mol Pharmacol* **46:**323–328.

Kohn KW, Ewig RAG, Erickson LC, and Zwelling LA (1981) Measurement of DNA strand breaks and cross-links by alcaline elution, in *DNA Repair: A Laboratory Manual of Research Procedures* (Friedberg EC and Hanawalt PC, eds) pp 379–401, Marcel Dekker, New York.

Koo H-M, Monks A, Mikheev A, Rubinstein LV, Gray-Goodrich M, McWilliams MJ, Alvord W, Oie HK, Gazdar AF, Paull KD, Zarbl H, and Vande Woude GF (1996) Enhanced sensitivity to 1-β-D-arabinofuranosylcytosine and topoisomerase II in-

hibitors in tumor cell lines harboring activated *ras* oncogenes. *Cancer Res* **56:** 5211–5216.
Kraus-Berthier L, Guilbaud N, Jan M, Saint-Dizier D, Rouillon MH, Burbridge MF, Pierré A, and Atassi G (1997) Experimental antitumor activity of S16020–2 in a panel of human tumors. *Eur J Cancer* **33:**1881–1887.
Lambert B, Jones BK, Roques BP, Le Pecq J-B, and Yeung AT (1989) The noncovalent complex between DNA and the bifunctional intercalator ditercalinium is a substrate for the UvrABC endonuclease of *Escherichia coli*. *Proc Natl Acad Sci USA* **86:**6557–6561.
Léonce S, Pérez V, Casabianca-Pignède M-R, Anstett M, Bisagni E, Pierré A, and Atassi G (1996) *In vitro* cytotoxicity of S16020–2, a new olivacine derivative. *Invest New Drugs* **14:**169–180.
Liu LF (1989) DNA topoisomerase poisons as antitumor drugs. *Annu Rev Biochem* **58:**351–375.
Liu LF and Miller KG (1981) Eukaryotic DNA topoisomerases: two forms of type I DNA topoisomerase from HeLa cell nuclei. *Proc Natl Acad Sci USA* **78:**3487–3491.
McGhee JD and von Hippel PH (1974) Theoretical aspects of DNA-protein interactions: co-operative and non-co-operative binding of large ligands to a one-dimensional homogeneous lattice. *J Mol Biol* **86:**469–489.
Pommier Y, Fesen M, and Goldwasser F (1996) Topoisomerase II inhibitors: the epipodophyllotoxins, m-AMSA, and the ellipticine derivatives, in *Cancer Chemotherapy and Biotherapy*, 2nd ed (Chabner BA and Longo DL, eds) pp 435–461, Lippincott-Raven, Philadelphia.
Pommier Y, Schwartz RE, Zwelling LA, Kerrigan D, Mattern MR, Charcosset J-Y, Jacquemin-Sablon A, and Kohn KW (1986) Reduced formation of protein-associated DNA strand-breaks in Chinese hamster cells resistant to topoisomerase II inhibitors. *Cancer Res* **46:**611–616.
Robinson MJ and Osheroff N (1991) Effects of antineoplastic drugs on the post-strand passage DNA cleavage/religation equilibrium of topoisomerase II. *Biochemistry* **30:**1807–1813.
Ross WE, Glaubiger DL, and Kohn KW (1979) Qualitative and quantitative aspects of intercalator-induced DNA strand breaks. *Biochim Biophys Acta* **562**:41–50.
Salles B, Charcosset J-Y, and Jacquemin-Sablon A (1982) Isolation and properties of Chinese hamster lung cells resistant to ellipticine derivatives. *Cancer Treat Rep* **66:**327–337.
Sambrook J, Fritsch EF, and Maniatis T (1989) *Molecular Cloning: A Laboratory Manual*, 2nd ed. Cold Spring Harbor Laboratory Press, Cold Spring Harbor, NY.
Saucier J-M, Festy B, and Le Pecq J-B (1971) The change of the torsion of the DNA helix caused by intercalation. II: Measurement of the relative change of torsion induced by various intercalating drugs. *Biochimie* **53:**973–980.
Sorensen BS, Sinding J, Andersen AH, Alsner J, Jensen PB, and Westergaard O (1992) Mode of action of topoisomerase II-targeting agents at a specific DNA sequence: uncoupling the DNA binding, cleavage and religation events. *J Mol Biol* **228:**778–786.
Worland ST and Wang JC (1989) Inducible overexpression, purification, and active site mapping of DNA topoisomerase II from the yeast *Saccharomyces cerevisae*. *J Biol Chem* 264:4412–4416.

Send reprint requests to: Dr. Jean-Marie Saucier, Unité de Recherche Associée au CNRS 147, Institut Gustave Roussy, 94805 Villejuif Cedex, France. E-mail: paucier@igr.fr